Journal of Power Sources 190 (2009) 307–310

Contents lists available at ScienceDirect

Journal of Power Sources

journal homepage: www.elsevier.com/locate/jpowsour

Short communication

# Preparation of dense and uniform $La_{0.6}Sr_{0.4}Co_{0.2}Fe_{0.8}O_{3-\delta}$ (LSCF) films for fundamental studies of SOFC cathodes

Jae-Wung Lee[a,b], Ze Liu[a,c], Lei Yang[a], Harry Abernathy[a], Song-Ho Choi[a], Hyoun-Ee Kim[b], Meilin Liu[a,*]

[a] School of Materials Science and Engineering, Georgia Institute of Technology, Atlanta, GA, 30332-0245, USA
[b] School of Materials Science and Engineering, Seoul National University, Seoul, 151-742, South Korea
[c] Union Research Center of Fuel Cell, School of Chemical & Environment Engineering, China University of Mining & Technology (CUMTB), Beijing, 100083, China

ARTICLE INFO

*Article history:*
Received 22 November 2008
Received in revised form 17 January 2009
Accepted 28 January 2009
Available online 6 February 2009

*Keywords:*
Cathode
LSCF
Sputtering
Thin film
SOFC

ABSTRACT

Thin films of $La_{0.6}Sr_{0.4}Co_{0.2}Fe_{0.8}O_{3-\delta}$ (LSCF) were deposited on (1 0 0) silicon and on GDC electrolyte substrates by rf-magnetron sputtering using a single-phase oxide target of LSCF. The conditions for sputtering were systematically studied to get dense and uniform films, including substrate temperature (23–600 °C) background pressure ($1.2 \times 10^{-2}$ to $3.0 \times 10^{-2}$ mbar), power, and deposition time. Results indicate that to produce a dense, uniform, and crack-free LSCF film, the best substrate temperature is 23 °C and the argon pressure is $2.5 \times 10^{-2}$ mbar. Further, the electrochemical properties of a dense LSCF film were also determined in a cell consisting of a dense LSCF film (as working electrode), a GDC electrolyte membrane, and a porous LSCF counter electrode. Successful fabrication of high quality (dense and uniform) LSCF films with control of thickness, morphology, and crystallinity is vital to fundamental studies of cathode materials for solid oxide fuel cells.



## 1. Introduction

Solid oxide fuel cells (SOFCs) are a desirable energy conversion system because of their high energy efficiency and excellent fuel flexibility. To be economically competitive, however, the operating temperature must be reduced so that less expensive materials may be used. To operate SOFCs at lower temperatures, more efficient cathode materials must be developed to reduce polarization loss due to oxygen reduction [1–5].

$La_{1-x}Sr_xCo_{1-y}Fe_yO_{3-\delta}$ (LSCF) has attracted much attention because of its higher ionic and electronic conductivity than LSM-based materials [6,7]. In addition to function as a cathode for SOFC, it is also an excellent current collector for fundamental study of other less conductive cathode materials [8]. For this application, it is imperative to fabrication LSCF in a thin film form with controlled density, uniformity, thickness, and morphology. Here we report our findings in searching for suitable conditions for preparation of high-quality $La_{0.6}Sr_{0.4}Co_{0.2}Fe_{0.8}O_{3-\delta}$ films using rf-magnetron sputtering.

## 2. Experimental

### 2.1. Preparation of LSCF target

The precursors used for the $La_{0.6}Sr_{0.4}Co_{0.2}Fe_{0.8}O_{3-\delta}$ (LSCF) target were strontium carbonate ($SrCO_3$, 98+%) and the oxides of lanthanum, cobalt, and iron ($La_2O_3$, 99.99%; CoO, 99%; $Fe_2O_3$, 99+%, all from Sigma–Aldrich). A mixture of the precursors in stoichiometric ratio was calcined at 1000 °C for 2 h to form the desired phase. The resulting LSCF powder was then uniaxially pressed into disk followed by sintering at 1325 °C for 5 h to obtain LSCF target with dimension of 2.5 mm in diameter and 5 mm in thickness.

### 2.2. Preparation of substrate

The (1 0 0) silicon wafers (from EL-CAT Inc.) were used as substrate for LSCF film deposition to facilitate the characterization of the microscopic features of the LSCF films (such as thickness, morphology, and uniformity). For evaluation of the electrochemical properties, LSCF films were deposited on a $Ce_{0.9}Gd_{0.1}O_{1.95}$ (GDC) electrolyte. The electrochemical cell based on GDC is fabricated as follows. The GDC pellets were prepared by pressing commercial GDC powder (SY, ULSA) uniaxially for 1 min. The pellets were sintered at 1450 °C for 5 h. The density of the pellets was about 98%

* Corresponding author.
*E-mail address:* meilin.liu@mse.gatech.edu (M. Liu).

0378-7753/$ – see front matter © 2009 Elsevier B.V. All rights reserved.
doi:10.1016/j.jpowsour.2009.01.090

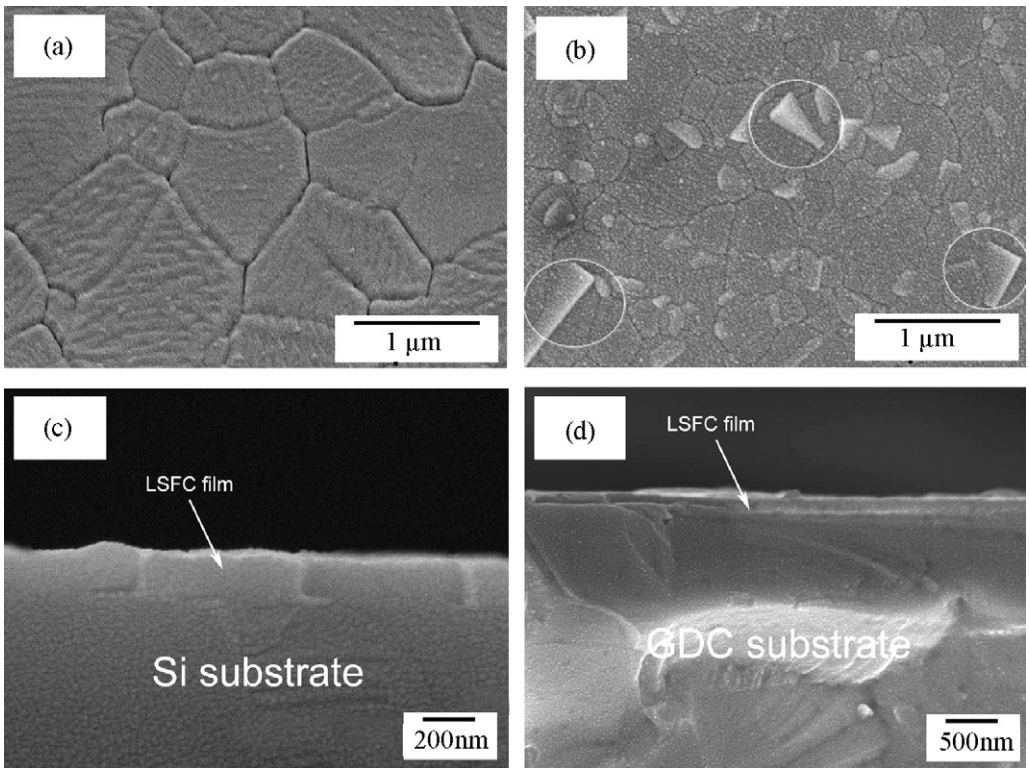


**Fig. 1.** SEM microstructures of LSCF film sputtered on Si substrate and on GDC bulk sample for 3 h at optimum pressure ($2.5 \times 10^{-2}$ mbar). (a) Surface view of LSCF film prepared at room temperature on Si substrate; (b) surface view of LSCF film prepared at 600 °C on Si substrate; (c) cross-section view of LSCF film prepared at room temperature for 3 h on Si substrate and (d) cross-section view of LSCF film prepared at room temperature for 3 h on GDC sample.

of the theoretical value as determined by the Archimedes' method. One side of the pellets was polished by MetPrep 3™ (Allied, High Tech Products Inc.), the other sides were brush painted with a $La_{0.6}Sr_{0.4}Co_{0.2}Fe_{0.8}O_{3-\delta}$ slurry, prepared by a citrate process [9]. The 30-μm thick porous LSCF cathode was fired at 1050 °C for 2 h.

### 2.3. Deposition of LSCF film

Thin films of LSCF were deposited on various substrates under different deposition conditions, including chamber pressure, working distance (or the distance between target and substrate), the type of gas, substrate temperature, and working power [10–13], Prior to deposition, the chamber was evacuated to a base pressure of $10^{-5}$ mbar. Argon was then leaked into the chamber to adjust the working pressure, which varied from $1.2 \times 10^{-2}$ to $3.0 \times 10^{-2}$ mbar. The temperature of the substrates was varied from room temperature to 600 °C. The rf power was kept at 20 W to avoid damage to the target. The LSCF films sputtered on a Si wafer or a GDC-based cell were then annealed at 800 °C for 1 h, with a heating and cooling rate of 10 °C $min^{-1}$. The LSCF films are used as the working electrode in electrochemical measurements.

### 2.4. Characterization of films

The morphology, microstructure, and thickness of the films were revealed using a scanning electron microscope (SEM; LEO 1530). The crystal structure and phase purity were analyzed using X-ray diffraction (XRD; X'Pert PRO Alpha-1) and Raman spectroscopy (Renishaw 1000, 2 mW 5 nm argon ion laser source). The electrochemical behavior of the test cells with LSCF film electrodes were tested using impedance spectroscopy (Solartron 1255 and 1287) in the frequency range of $10^{-3}$ to $10^{7}$ Hz.

## 3. Results and discussion

We systematically studied the effects of working pressure, working distance, and working power on deposition rate [10,11] as well as the effect of substrate temperature and chamber pressure on the microstructures of the deposited films [12,13]. Since the deposition rate of oxide films is much lower than that of metallic films, it is important to develop a set of parameters for fast deposition of LSCF films with desired microstructures (density, uniformity, and grain size).

Shown in Fig. 1(a) is a typical surface view of a LSCF film. While the morphology and microstructure appear to be insensitive to chamber pressure, the deposition rate was greatly altered by the working pressure.

Shown in Fig. 2 is the dependence of deposition rate on chamber pressure. In the pressure range studied (from $1.2 \times 10^{-2}$ to $3.0 \times 10^{-2}$ mbar), the deposition rate reached a maximum at $2.5 \times 10^{-2}$ mbar of argon. This is because, on one hand, the rate of bombardment of the target by argon atoms increases with the chamber pressure; on the other hand, the mean free path between elastic collisions for the sputtered element decreases with pressure as the element collides more often with argon atoms [14].

The sputtering pressure was then kept at $2.5 \times 10^{-2}$ mbar (of argon) to achieve high deposition rate for subsequent studies.

LSCF films were deposited on substrate heated to different temperatures, from room temperature to 600 °C. Fig. 1(a) shows the surface morphology of a film prepared at room temperature and optimum pressure. It shows a dense and crack-free film with well-developed grain structure. The average grain size is around 1 μm. Films deposited on substrates at 600 °C had smaller grains and less uniform, as shown in Fig. 1(b). The circled grains appear to be some abnormal grains with distinct facets (e.g., a square-like shape). LSCF tends to form crystalline grains during sputtering, activated

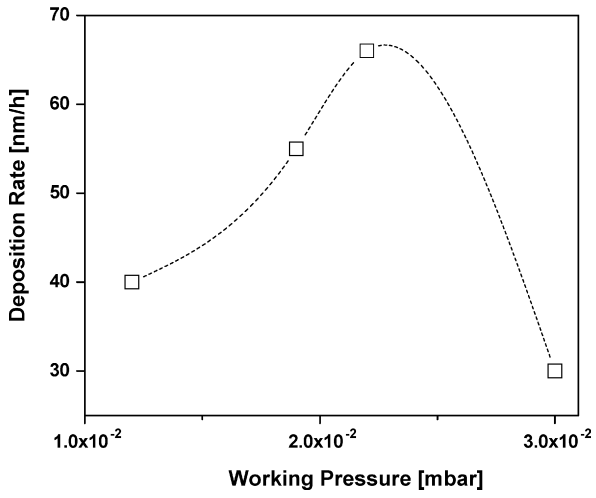


**Fig. 2.** LSCF film deposition rate as function of working pressure.

by energy from the heated substrate. It appears that the number of heterogeneous nucleation sites also increased with substrate temperature, producing smaller grain sizes at higher substrate temperature than at room temperature [15,16].

Fig. 1(c) shows a cross-sectional view of an LSCF film prepared on Si at $2.5 \times 10^{-2}$ mbar and room temperature for 3 h. It has a well-developed columnar structure with a thickness around 150 nm. The average column diameter is around 500 nm, which can also be seen from the surface view shown in Fig. 1(a). Fig. 1(d) shows a cross-sectional view of an LSCF film prepared on a GDC electrolyte substrate at optimum pressure and room temperature for 3 h. The LSCF film was well adhered to the GDC surface.

The crystal structure and phase composition of the LSF films and the LSCF target were analyzed using XRD and Raman spectroscopy. Fig. 3 shows Raman spectra of the LSCF target and an LSCF film on (1 0 0) Si wafer collected using 514 nm laser. Raman spectroscopy of LSCF target was measured for comparison with LSCF film. In the case of the target, two characteristic peaks are observed around 545 and 635 $cm^{-1}$. The Raman spectra for the LSCF film exhibited similar peaks, with the 545 $cm^{-1}$ peaks being masked by the very strong $F_2$ peak from the silicon substrate at 520 $cm^{-1}$. The 960-$cm^{-1}$ peak from the LSCF film sample is also

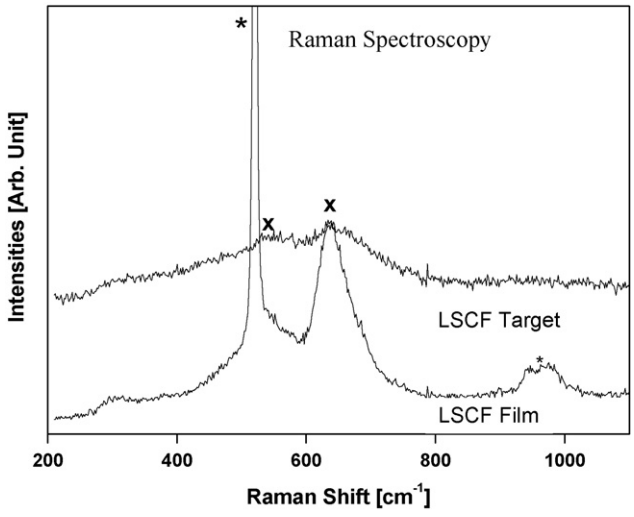


**Fig. 3.** Raman spectra of LSCF thin film deposited on Si substrate, and the other two peaks marked with (×) are assigned to the LSCF film and target. The two peaks marked with (*) are assigned to the Si substrate.

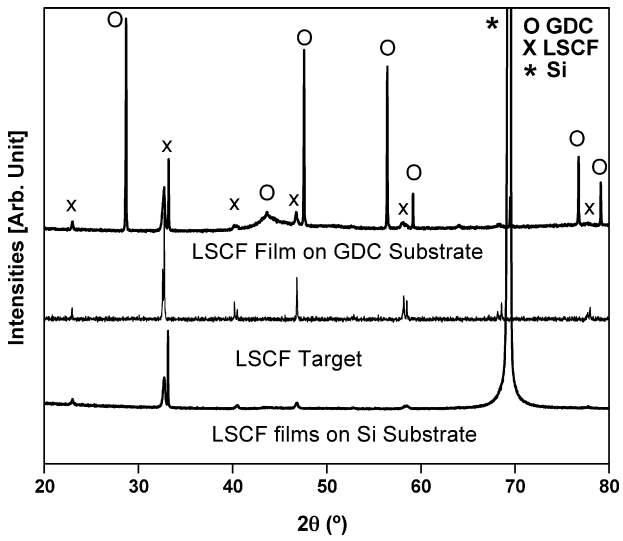


**Fig. 4.** XRD patterns of the LSCF films sputtered at optimum condition on Si and GDC substrate after annealing and LSCF target. The peaks marked with (×) and (○) are assigned to LSCF and GDC, respectively. And the peaks marked with (*) are assigned to the Si substrate.

from the Si substrate. Shown in Fig. 4 are the X-ray diffraction patterns of the LSCF target, an LSCF film on Si substrate, and an LSCF film on GDC substrate (both films were annealed at 800 °C for 1 h).

The optimal annealing temperature for the LSCF films, 800 °C, is about 2/3 of the sintering temperature for LSCF bulk samples [3]. Comparing with LSCF target, the LSCF film appears to be well prepared on Si substrate [16,17]. There is no observable reaction between LSCF film and Si substrate according to both XRD pattern and Raman spectra. Similarly, LSCF films on GDC electrolyte substrates are also well prepared, as shown in Fig. 4 [18,19].

It is noted that the Raman peaks for the LSCF film (flat crystals as seen in Fig. 1(c)) on a silicon substrate appear much sharper than those for the LSCF target (a 3-mm thick polycrystalline pellet). However, the factors that determine the sharpness of these Raman peaks are still under investigation, including the geometry and quality of the crystalline samples and the nature of the substrate.

Shown in Fig. 5(a) are some typical impedance spectra of a cell with a dense LSCF film electrode (~200 nm), a GDC electrolyte membrane, and a porous LSCF counter electrode, as measured in air at 600–800 °C. The intercepts of the impedance loops with the real axis at high frequencies represent the bulk resistances of the GDC electrolyte whereas the differences in the intercepts (with the real axis) at low and high frequencies (or the spans of impedance loops) correspond to the polarization resistances of the dense LSCF film electrode, which varied from 122 to 4.5 $\Omega\,cm^2$ as temperature was increased from 600 to 800 °C (while the impedances of the porous LSCF electrodes were less than 0.1 $\Omega\,cm^2$) [20,21].

Careful analysis of the impedance data for the dense LSCF film electrodes using our continuum models developed for dense mixed-conducting cathode [22] suggest that the larger impedance loop (occurred at low frequencies) represents the impedance to surface oxygen exchange reaction whereas the smaller impedance loop (occurred at higher frequencies) corresponds to the impedance to vacancy transfer across the interface between the LSCF electrode and the GDC electrolyte. Shown in Fig. 5(c) are the resistance to surface exchange reaction, $R_1$, and the resistance to vacancy transfer across the GDC/LSCF interface, $R_2$, extracted from the impedance data using curve fitting to an equivalent circuit. The values for both $R_1$ and $R_2$ at 750 °C are in reasonable agreement with those reported in the literature for similar systems [23]. Clearly, the dominant resis-

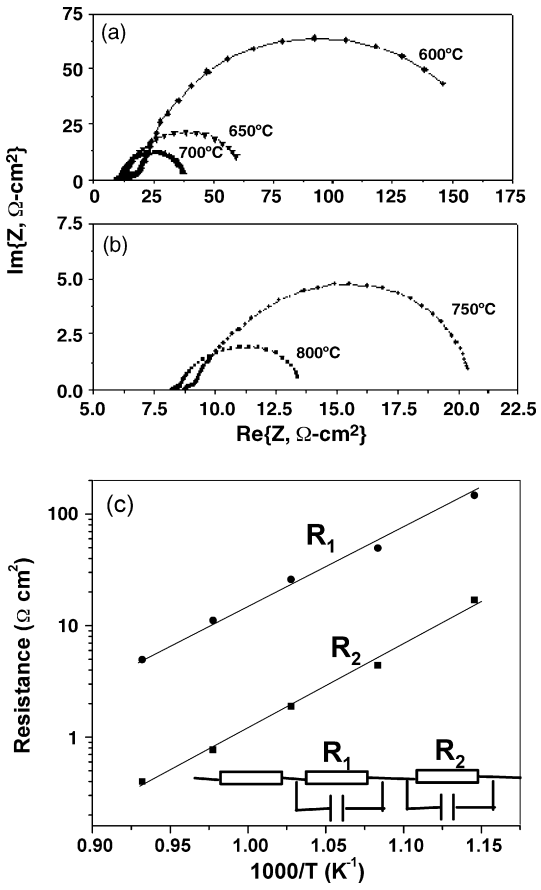


**Fig. 5.** (a) and (b) some typical impedance spectra of a single cell with a configuration of *dense LSCF film*|*GDC electrolyte*|*porous LSCF*. The electrode polarization resistance of the entire cell is dominated by the polarization resistance of the dense LSCF film since the polarization resistance of the porous LSCF counter electrode is orders of magnitude smaller than that of the dense LSCF film. (c) The resistance to surface exchange reaction occurred a low frequencies, $R_1$, and the resistance to vacancy transfer across the GDC/LSCF interface occurred a high frequencies, $R_2$, extracted from the impedance data using curve fitting to an equivalent circuit.

tive process is the oxygen reduction processes occurring on the surface of the dense LSCF film electrode (~200 nm thick). When the LSCF film is sufficiently thick, the mass transport through the dense film will become dominating. Thus, LSCF films of deferent thicknesses can be used for systematic investigate into the details of the surface catalytic and bulk transport properties of LSCF films under different electrochemical conditions. For example, the polarization resistance can be measured as a function of the film thickness, the partial pressure of oxygen, and the amplitude of dc polarization, from which the surface catalytic properties and the transport properties of the dense LSCF film may be deduced. This approach can be used to study the catalytic and transport properties of other mixed-conducting materials as cathode for SOFCs.

## 4. Conclusions

Dense, crack-free, and uniform LSCF films have been successfully deposited on Si and GDC electrolyte substrates. Results suggest that a high deposition rate was achieved at argon pressure of $2.5 \times 10^{-2}$ mbar at room temperature. Upon annealing at 800 °C for 1 h, the LSCF films develop a crystalline structure with high phase purity. The electrical properties of the LSCF films were examined in a cell with a configuration of LSCF film/GDC/porous LSCF using impedance spectroscopy. The test cell with a dense LSCF film can be used for fundamental study of catalytic properties of mixed-conducting cathode materials.

## Acknowledgment

This work was supported by the U.S. Department of Energy SECA core technology program under Grant No. DE-NT-0006557.

## References

[1] N.Q. Minh, T. Takahashi, Science and Technology of Ceramic Fuel Cell, Elsevier, New York, 1995, p. 1.
[2] R.M. Ormerod, Chem. Soc. Rev. 32 (2003) 17–28.
[3] A.J. McEvoy, Solid State Ionics 132 (2000) 159–165.
[4] Y. Liu, S. Zha, M. Liu, Adv. Mater. 16 (2004) 256–260.
[5] C.R. Xia, M. Liu, Adv. Mater. 14 (2002) 521–523.
[6] Y. Teraoka, H.M. Zhang, K. Okamoto, N. Yamazoe, Mater. Res. Bull. 23 (1988) 51.
[7] F. Prado, N. Grunbaum, A. Caneiro, A. Manthiram, Solid State Ionics 167 (2004) 147.
[8] R.K. Gupta, E.Y. Kim, H.S. Noh, C.M. Whang, J. Phys. D: Appl. Phys. 41 (2008) 032003.
[9] Z. Liu, M.F. Han, W.T. Miao, J. Power Source 173 (2) (2007) 837–841.
[10] Movchan, Demchisn, Phys. Met. Metallogr. 28 (1969) 83.
[11] J.A. Thornton, JVST 11 (1974) 666.
[12] K.H. Muller, J. Appl. Phys. 58 (1985) 2573.
[13] J.E. Greene, C. Wickersham, J. Appl. Phys. 47 (1976) 3636.
[14] J.E. Greene Sputter, Deposition, 1989, chapter 5, 11.
[15] C.V. Thompson, Ann. Rev. Mater. Sci. 20 (1990) 245.
[16] S.J. Zheng, K. Dua, X.L. Ma, J. Eur. Ceram. Soc. 28 (2008) 1821.
[17] A. Afshara, A. Simchi, Scripta Mater. 58 (2008) 966.
[18] G. Corbel, S. Mestiri, P. Lacorre, Solid State Sci. 7 (2005) 1216.
[19] L. Qiu, T. Ichikawa, A. Hirano, N. Imanishi, Y. Takeda, Solid State Ionics 158 (2003) 55.
[20] B.C.H. Steele, Solid State Ionics 129 (1–4) (2000) 95–110.
[21] J. Fleig, F.S. Baumann, V. Brichzin, H.R. Kim, J. Jamnik, G. Cristiani, H.U. Habermeier, J. Maier, Fuel Cells 3–4 (2006) 284–292.
[22] M.E. Lynch, D.S. Mebane, Y. Liu, M. Liu, J. Electrochem. Soc. 155 (2008) B635–B643.
[23] F.S. Baumann, et al., Solid State Ionics 177 (2006) 1071–1081.